SOURCE STRUCTURE ERRORS IN THE SYNCHRONIZATION OF CLOCKS BY RADIO INTERFEROMETRY

J. B. Thomas
Jet Propulsion Laboratory, Pasadena, California

ABSTRACT

Radio interferometry has the potential of synchronizing clocks across intercontinental distances with accuracies better than one nanosecond. One of the potential error sources in such determinations is the spatial structure of the natural radio sources that provide the reference signals. Due to their extent, the effective position of these sources can vary as a function of the length and orientation of the baseline vector joining the two antennas. If they are not corrected, such variations can lead to errors in clock synchronization. This presentation discusses the theory of structure corrections and gives specific examples to illustrate the nature and size of the effect.

INTRODUCTION

Radio interferometry with natural radio sources has the potential for very accurately synchronizing clocks over distances up to intercontinental lengths, possibly eventually reaching accuracies of the order of 0.1 nsec. Comparisons of absolute clock synchronization by interferometry with the measurements obtained by traveling clocks have already been carried out at the 10-20 nsec level by the MIT VLBI group and at the 5 nsec level by the JPL VLBI group (see L. E. Young's presentation in this conference). One of the error sources that can degrade high accuracy synchronization measurements is the extended structure of the natural sources. In this talk, I will present the results of a study to estimate the size of this particular error source. Before the results of that study are outlined, a few slides of background explanation will be presented for those unfamiliar with the source structure problem.

INTERFEROMETRY THEORY

The first slide is a schematic representation of the basic geometry of the interferometry process and defines the baseline vector, source direction, and geometric delay. Given two antennas, the basic idea is to measure the difference in arrival times of a radio signal from a natural source. After appropriate calibrations, the measured delay will be equal to the geometric delay plus a clock synchronization offset. If the geometric delay can be removed on the basis of a priori knowledge of source direction, earth orientation, etc., then the offset between station clocks can be extracted. If the position of the source is uncertain due to extended structure, clock synchronization determinations will be impaired.

This same slide also presents the first step of the data reduction procedure used to extract delay. The analysis has been reduced to an ideal form and includes a simplified derivation of the fringes that would be obtained by perfect instrumentation when a monochromatic signal is recorded for a point source. A sinusoidal voltage signal is recorded at both stations but the signal at station 2 is offset in time by the geometric delay τ_g and by a clock synchronization error τ_c (relative to station 1). The signals recorded at the two stations are multiplied together (cross-correlated) to produce the sinusoidal cross-correlation function referred to as fringes. The fringe phase is extracted by post-correlation software and is equal to a product of observing frequency and $\tau_g + \tau_c$. As shown in the next slide (2), when the phase is observed at two frequencies (separated by about 40 MHz in JPL efforts), the two phase values can be combined as indicated to obtain the observed delay τ_{BWS}. Integer cycle ambiguities in τ_{BWS} resulting from phase ambiguities can be removed on the basis of a priori information and/or the delays from other more closely spaced channel pairs. The resulting delay will be referred to as the bandwidth synthesis (BWS) delay. As indicated, the synchronization offset is obtained by subtracting from the BWS delay an a priori model for geometric delay. Synchronization measurements can be no more accurate than the accuracy of this geometric model. If the source is extended, the specification of source position, and therefore geometric delay, becomes uncertain.

To begin to explain structure effects, it is useful to present a simplified derivation of the fringes for a double-point source. As we shall see, these results can then be easily generalized

to an arbitrary brightness distribution. As shown in the next slide (3), suppose two points in the sky radiate with power a_1^2 and a_2^2 at positions $\hat{S}$ and $\hat{S}'$. If the points radiate uncorrelated signals, the observed fringes will be the sum of the fringe expressions separately derived for each point (see slide 1). As shown, the sum can be rewritten as a product of a modulating factor R and the fringes from point source 1. The factor R depends on the difference of the source vectors $(\hat{S}' - \hat{S})$ and varies as a function of baseline $\vec{B}$, ranging between summed power $(a_1^2 + a_2^2)$ and difference power $(a_1^2 - a_2^2)$. Remember the form of these terms in R - power times a phasor - since they will be used later to generalize to an arbitrary distribution.

As suggested in the present slide (3) and stated in the next slide (4), the maximum constructive interference occurs when the difference in geometric delay for the two points is equal to an integral number of wavelengths of the observed signal. If the position difference $(\vec{\delta S} = \hat{S}' - \hat{S})$ is converted into an angular differential representing the corresponding change in angle (ψ) between baseline vector and source detection, one obtains an expression for the angular separation of adjacent lines on the celestial sphere between which constructive interference of source emissions would occur. (The meaning of δS is changed here to denote the vector difference between two possible points of radio emission on the celestial sphere). These lines are usually referred to as fringes on the sky. Note that, as baseline length increases or as wavelength decreases, the spacing of the sky fringes decreases. Further, minimum fringe spacing occurs when the source direction is perpendicular to the baseline vector ($\psi = 90^\circ$). For B = 10,000 km and λ = 3.5 cm (f = 8.5 GHz), the minimum fringe spacing (maximum resolution) is 3.5 nrad (0".0007).

The next slide (5) schematically shows the changes in effective position for a hypothetical extended source as baseline length changes. The source is assumed to consist of a point source placed next to a diffuse component. For the short baseline, the fringe spacing is large compared to the size of the source. Since all components contribute to the cross-correlation without destructive interference, the effective source position will

be equal to the centroid of the two components. For the long baseline, the fringe spacing decreases so much that the diffuse component is much larger than the fringe spacing and different parts of that component destructively interfere with one another. Consequently, this component is "resolved out" to such an extent that it effectively does not contribute to cross-correlation. Thus, for the long baseline, the effective position moves and becomes the position of the point component. This example emphasizes the possible dependence of effective source position on baseline length and orientation.

As summarized on the next slide (6), one can easily generalize the analysis for the double-point source to an arbitrary brightness distribution. By adding more points to the sum in slide 3, and then converting the sum to an integral, one obtains the factor R for the general distribution. The factor R, usually referred to as the brightness transform or complex visibility function, becomes the complex Fourier transform of the brightness distribution. The reference position $\hat{S}_o$, which was placed at the strongest point for a double-point source, is arbitrary at this point, provided it is near the source.

The next slide (7) shows how structure phase ϕ_B and fringe amplitude are defined from the complex brightness transform. When total fringe phase is measured, this structure phase will be one of the components. As shown in slide 2, the observed BWS delay is essentially the derivative of phase w.r.t. frequency. Thus the contribution of structure to the measured BWS delay will be approximately given by the partial of ϕ_B w.r.t. frequency. Such partials can be readily obtained for both analytical and measured (numerical) source distributions.

The next slide (8) presents without derivation the equation for computing the effective position of a source, given a brightness distribution independent of time and frequency. For computational convenience, the effective position is computed relative to an assigned reference position $\hat{S}_o$. One can show that, for a given observation, the extended source can be analytically replaced by a point source located at the effective position. With this and only this assigned position, the hypothetical point source will produce the same geometric delay and geometric delay rate as the actual source when the BWS delay and phase-delay rate are the observables.

As can be seen, the effective position is a relative of the ordinary centroid but is based on the quadrature components of the resolved distribution. Given a measured brightness distribution, this expression for effective position can be readily evaluated. One can easily show that the effective position becomes the ordinary centroid when the baseline approaches zero, as one would expect.

Before structure effects can be properly removed in clock synch measurements based on a single source, the absolute location of the brightness distribution for that source must be accurately determined relative to a global set of celestial coordinates. When obtained through multibaseline VLBI measurements, the brightness distribution for a source will be accurately determined relative to a set of local coordinates (structure coordinates) specific to that source but will not be accurately placed on the celestial sphere in one absolute sense. Accurate absolute positions are usually obtained by multiparameter fits to the delay values for many sources, where the delays are obtained through VLBI measurements independent of the structure measurements. For these solve-for locations to have meaning relative to the brightness distribution, each observation of delay for a given source must be corrected for the difference between effective position and some constant reference position, where both are computed in structure coordinates. The solve-for position of the source will then be the absolute location of the reference position for that source.

TWO EXAMPLES OF ANALYTICAL SOURCES

For the first example, the next slide (9) derives equations for the structure effects of a double-point source. As can be seen from slide 3, the brightness transform can be rewritten as a function of only two variables: the relative strength (g_2) of point source 2 and the projected separation (p) of the two sources in units of resolution. Both the phase and delay effects of structure become a function of these same two parameters. As explained in previous slides, the delay is obtained by taking the partial of phase w.r.t. frequency, but, for brevity, this operation is not shown.

The next slide (10) shows how the effective position of a double-point source varies as a function of p (the projected source separation in units of resolution) for selected ratios of the

point strengths. The plot can be constructed in this manner due to the fact that the effective position of a double-point source always lies on the line drawn through the two points. As shown, the effective position is equal to the ordinary centroid when the resolution is large compared to the source extent (i.e. when p = 0). As the resolution improves (i.e. as Δ decreases so that p increases), the effective position moves away from the ordinary centroid and can move far outside the extent of the source. In fact, for nearly equal point strengths, the effective position approaches infinity when p = integer/2. These nearly singular points correspond to points of large delay excursion as will be shown in the next slide.

This slide (11) plots the delay effect for a double-point source as a function of the same two parameters. The plotted values are referenced to the brightness centroid of the source rather than to the brightest component. This shift, which is not derived here, results in the subtraction of a simple term from the phase expression in slide (9). As can be seen in the plot, there can be critical values of baseline vector for which the delay effect becomes very large, even approaching infinity if the source strengths are nearly equal. These singular points occur when the component phasors sum to zero so that small changes in p can produce large changes in phase. These undesirable regions can be eliminated to a large extent by placing a lower limit on relative fringe amplitude. When the weaker source is 0.95 of the strength of the stronger source, the maximum delay effect at 8.5 GHz is 1.2 nsec for p = 0.5 cycle. This plot indicates that, except for the unusual case of very nearly equal point strengths, the structure effect of a double point source would be small relative to the present VLBI clock synchronization capabilities ($\sim$5 nsec). However, when clock synch accuracy reaches 0.1 nsec, structure effects will be very important.

For the second example, the next slide (12) presents the equations for the structure effects of a triple-point source. Note that phase and delay effects can be expressed as a function of four variables: the relative strengths (g_2, g_3) of point sources 2 and 3 and the two variables (p, q) that give the projected separations (in units of resolution) of point sources 2 and 3. When parametrized in this manner, the delay results can be used for any triple-point source with the specified values for (g_2, g_3) regardless of the point separations and directons. Two cases will be shown to illustrate typical delay behavior

for a triple-point source. The next slide (13) presents the first case and plots delay as a function of p and q for the strength values $g_2 = 0.2$ and $g_3 = 0.4$. Note that there are extrema in delay that occur with lattice-like regularity. It can be easily shown that these extrema correspond to points of minimum fringe amplitude. The extrema occur when p and q are multiples of 0.5, provided $g_2 + g_3 < 1$. For the example in this slide, the first delay extremum reaches 0.1 nsec at $p = q = 0.5$.

The next slide (14) presents the second case and shows the structure delay associated with a triple-point source with relative strength values $g_2 = 0.4$ and $g_3 = 0.8$. There are local regions in the (p, q) plane where the structure delay becomes very large and even certain points where it approaches infinity. In this slide, the delays are truncated above 1 nsec to improve the plots. As suggested by the sharp dips near the positive peaks, the delay goes to negative infinity next to each point of positive infinity. This behavior is demonstrated in the next slide (15) where the delay is inverted. These singular points occur whenever the amplitude drops to zero. One can easily show by means of three-phasor sums that, if $g_2 + g_3 \geq 1$, singular points can always be found on a lattice of points in the (p, q) plane. (We assume here that point source 1 has the greatest flux). One beneficial characteristic of such singular regions is that they can always be detected (and therefore avoided in large measure) through a drop in amplitude. Note that, in the regions between adjacent null points, the delay effect reaches 0.3 - 1.0 nsec for the plotted range of (p, q).

SUMMARY AND CONCLUSIONS

The analytical examples presented here indicate that, if a source can be accurately represented by a double-point or triple-point model, it might be necessary to avoid certain critical values of the baseline vector. At the critical points, the delay effect can even theoretically approach infinity for a pure multipoint source. The effective position at these points can move far outside the extent of the source. However it is unusual for a real source to consist solely of two or three sharp points. Real distributions tend to possess extended component rather than point features and usually have additional weaker components or background features. These characteristics would blunt the truly singular behavior found in pure multipoint models. Nevertheless, it seems likely that the structure effect in BWS delay will

be of the order of 0.5 nanosecond for some real sources at some baseline values. At the nanosecond level, structure effects would be small compared to present VLBI clock synch capabilities ($\sim$ 5 nsec). When VLBI clock synch reaches the 0.1 nsec level, structure effects are likely to become an important consideration.

The analysis presented here has concentrated on the BWS-delay observable. Unlike BWS delay, phase delay does not diverge to infinity near points of zero amplitude. In such cases, the phase-delay observable will be subject to less extreme structure errors than BWS delay. Therefore, even though the development of a phase-delay system is more difficult, the phase-delay observable has important advantages with regard to structure effects.

In order to obtain a more accurate assessment of structure effects, an effort is underway to analyze measured brightness distributions for a number of real sources. That study will help to assess the feasibility of limiting the size of structure effects through judicious selection of sources and/or through enforcement of a lower limit on relative fringe amplitude.

ACKNOWLEDGEMENTS

I would like to thank Sue Finley for her enthusiastic assistance in generating the three-dimensional computer plots of structure delay for a triple-point source. This paper presents the results of one phase of research carried out at the Jet Propulsion Laboratory, California Institute of Technology, under contract No. NAS 7-100, sponsored by the National Aeronautics and Space Administration.

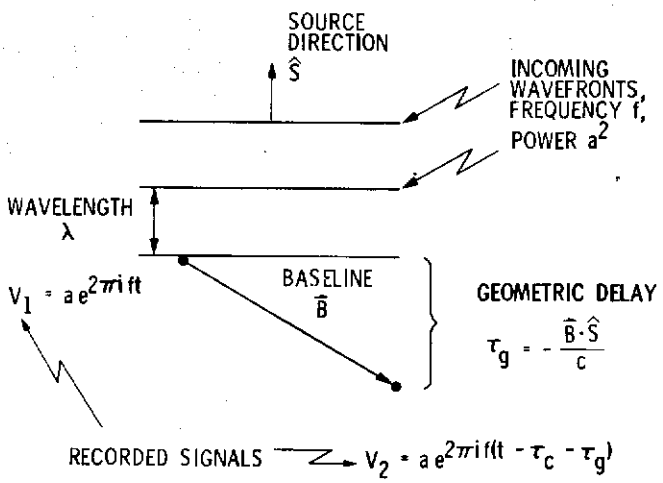

CROSS-CORRELATE TO OBTAIN FRINGES:

$$V_1 V_2^* = a^2 e^{2\pi i f(\tau_c + \tau_g)}$$

Figure 1. Interferometry with Perfect Instrumentation, Point Source & Monochromatic-Signal

PHASE EXTRACTED FROM FRINGES:

$$\phi = f(\tau_c + \tau_g) \quad \text{AT FREQUENCY } f$$

$$\phi' = f'(\tau_c + \tau_g) \quad \text{AT FREQUENCY } f'$$

COMPUTE DELAY FROM PHASE:

$$\tau_{BWS} = \frac{\phi' - \phi}{f' - f} = \tau_c + \tau_g$$

USE A PRIORI TO EXTRACT CLOCK SYNCH:

$$\tau_c(\text{obs}) = \tau_{BWS} - \tau_g \text{ (model)}$$

Figure 2. Phase, Delay and Clock Synch from VLBI

GIVEN TWO POINTS WITH POSITIONS ($\hat{S}$, $\hat{S}'$) AND STRENGTHS (a_1^2, a_2^2)

GEOMETRIC DELAYS:

$$\tau_g = -\vec{B}\cdot\hat{S}/c \qquad \tau_g' = -\vec{B}\cdot\hat{S}'/c$$

FRINGES FROM CROSS-CORRELATION:

$$V_1 V_2^* = a_1^2\, e^{2\pi i f(\tau_c + \tau_g)} + a_2^2\, e^{2\pi i f(\tau_c + \tau_g')}$$

$$= R\; e^{2\pi i f(\tau_c + \tau_g)}$$

WHERE

$$R \equiv a_1^2 + a_2^2\, e^{-2\pi i f\, \vec{B}\cdot\delta\vec{S}/c}$$

$$\delta\vec{S} = \hat{S}' - \hat{S}$$

Figure 3. Fringes for a Double-Point Source

AMPLITUDE $|R|$ = MAXIMUM WHEN

$$f\,\vec{B}\cdot\delta\vec{S}/c = \text{INTEGER}.$$

IF

$$\vec{B}\cdot\hat{S} = B\cos\psi$$

SO THAT

$$\vec{B}\cdot\delta\vec{S} = -B\sin\psi\,\delta\psi$$

THEN FRINGE SPACING (RESOLUTION) BECOMES

$$\boxed{\Delta = \frac{\lambda}{B}\,\frac{1}{\sin\psi}}$$

Figure 4. Fringes on the Sky

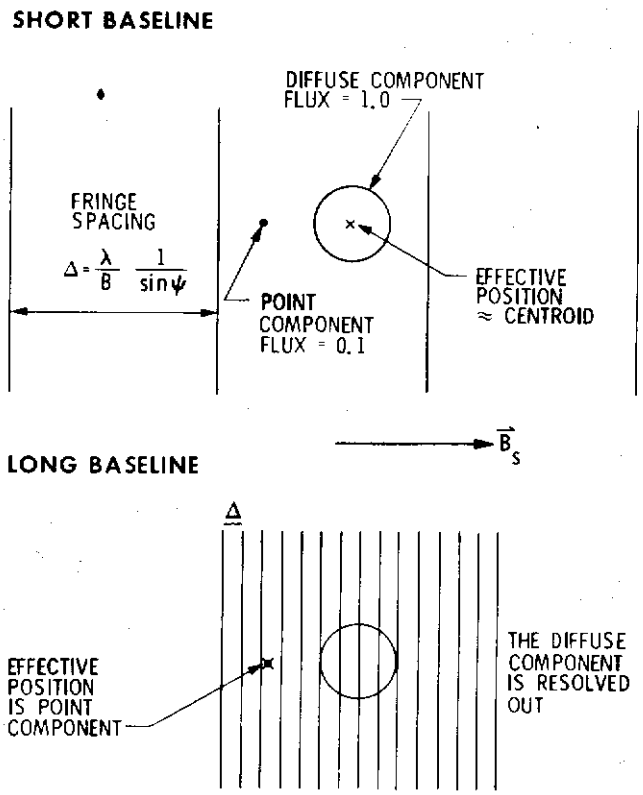

Figure 5. Schematic Example of Effective Position

FOR GENERAL SOURCE

$$R\left(\frac{\vec{B}_s}{\lambda}\right) = \iint D(\hat{S})\, e^{-2\pi i \vec{B}_s \cdot \delta\vec{S}/\lambda} d\Omega_{\delta\vec{S}}$$

WHERE

$D(\hat{S})$ = BRIGHTNESS DISTRIBUTION

$d\Omega_{\delta\vec{S}}$ = "AREA" DIFFERENTIAL ON PLANE OF SKY

$\delta\vec{S} = \hat{S} - \hat{S}_0$

$\hat{S}_0$ = ASSIGNED REFERENCE POSITION

$\vec{B}_s$ = SKY-PROJECTED BASELINE VECTOR

Figure 6. The Brightness Transform

REWRITE BRIGHTNESS TRANSFORM

$$R = |R| e^{i2\pi\phi_B}$$

WHERE

$|R|$ = FRINGE AMPLITUDE

ϕ_B = STRUCTURE PHASE

STRUCTURE EFFECT ON τ_{BWS}:

$$\Delta\tau \approx \frac{\partial\phi_B}{\partial f}$$

Figure 7. Structure Phase and Delay

$$\langle\delta\vec{S}\rangle_E = \frac{Z_c^2\langle\delta\vec{S}\rangle_c + Z_s^2\langle\delta\vec{S}\rangle_s}{Z_c^2 + Z_s^2}$$

WHERE

$$\langle\delta\vec{S}\rangle_c \equiv \frac{1}{Z_c}\int \delta\vec{S}\, D(\hat{S})\, \cos(2\pi\vec{B}_s \cdot \delta\vec{S}/\lambda)\, d\Omega_{\delta\vec{S}}$$

$$\langle\delta\vec{S}\rangle_s \equiv \frac{1}{Z_s}\int \delta\vec{S}\, D(\hat{S})\, \sin(2\pi\vec{B}_s \cdot \delta\vec{S}/\lambda)\, d\Omega_{\delta\vec{S}}$$

$$\delta\vec{S} = \hat{S} - \hat{S}_0$$

$(Z_c, -Z_s)$ = (REAL, IMAG) PART OF BRIGHTNESS TRANSFORM

*FOR BWS DELAY AND PHASE-DELAY RATE

Figure 8. Computation of Effective Position* from the Brightness Distribution

REWRITE EARLIER RESULT AS

$$R \propto 1 + g_2 \, e^{-i 2\pi p}$$

WHERE

$$g_2 \equiv a_2^2 / a_1^2 \qquad \text{AND} \qquad p \equiv \hat{B}_s \cdot \delta\vec{S}/\Delta$$

FOR WHICH $\Delta \equiv \dfrac{\lambda}{B \sin \psi}$ = RESOLUTION

$\hat{B}_s$ = UNIT SKY-PROJECTED BASELINE VECTOR

STRUCTURE PHASE BECOMES

$$\phi_B = \tan^{-1}\left[\frac{-g_2 \sin 2\pi p}{1 + g_2 \cos 2\pi p}\right]$$

Figure 9. Structure Effect for a Double-Point Source

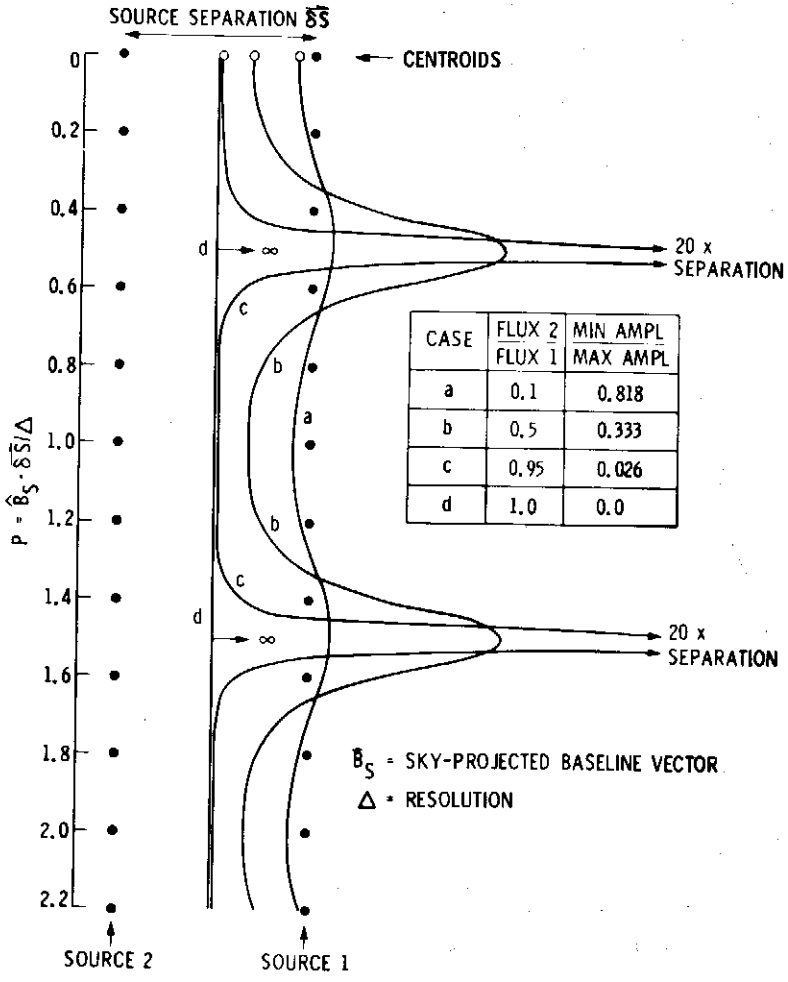

Figure 10. Effective Position for Frequency-Independent Double-Point Source: BWS Delay and Delay Rate

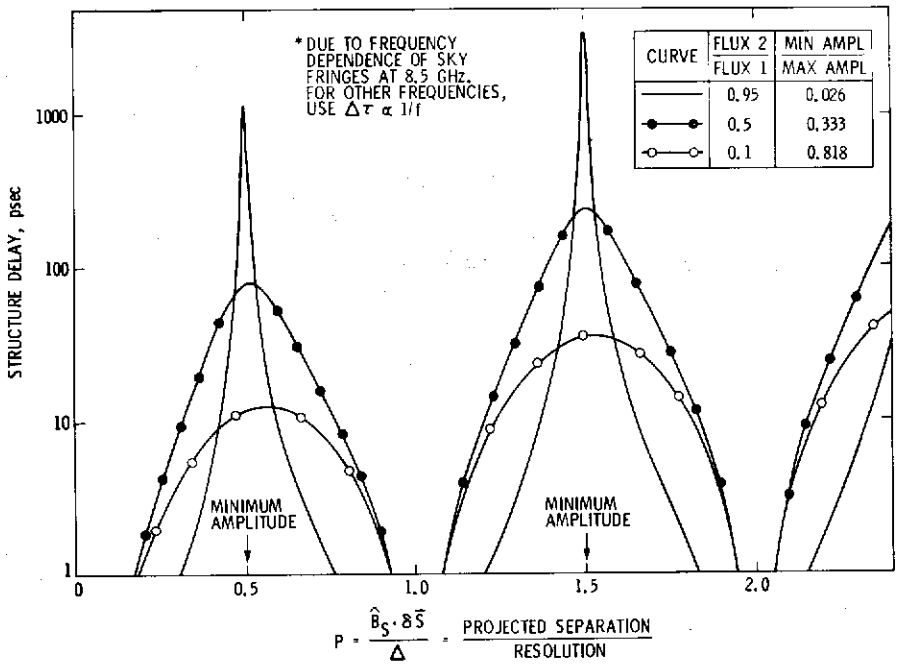

Figure 11. BWS Delay* Relative to Brightness Centroid for Double-Point Source

IN ANALOGY WITH DOUBLE-POINT SOURCE

$$R = 1 + g_2 e^{-i2\pi p} + g_3 e^{-i2\pi q}$$

WHERE

$$p = \frac{\hat{B}_s \cdot \delta\vec{S}_2}{\Delta} \qquad q = \frac{\hat{B}_s \cdot \delta\vec{S}_3}{\Delta}$$

AND

$$\delta\vec{S}_K \equiv \hat{S}_K - \hat{S}_1 \qquad g_K \equiv a_K^2 / a_1^2$$

STRUCTURE PHASE BECOMES

$$\phi_B = \tan^{-1}\left[\frac{-g_2 \sin 2\pi p - g_3 \sin 2\pi q}{1 + g_2 \cos 2\pi p + g_3 \cos 2\pi q}\right]$$

Figure 12. Structure Effect for a Triple-Point Source

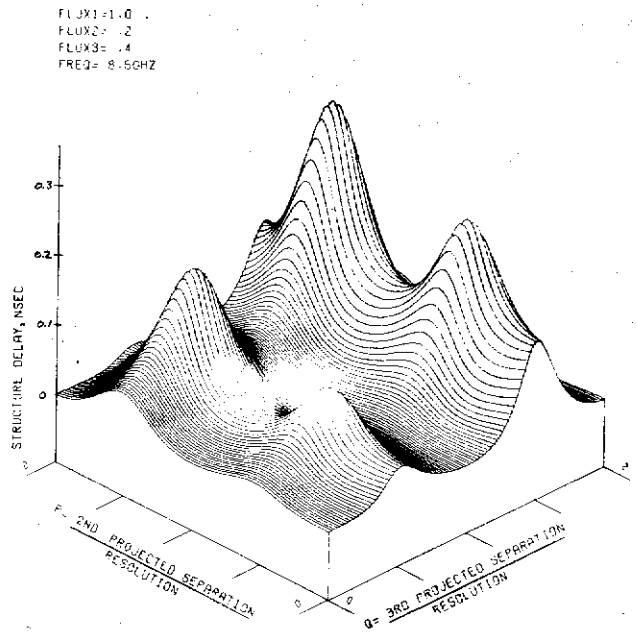

Figure 13. BWS Delay Relative to Brightness Centroid for a Triple-Point Source

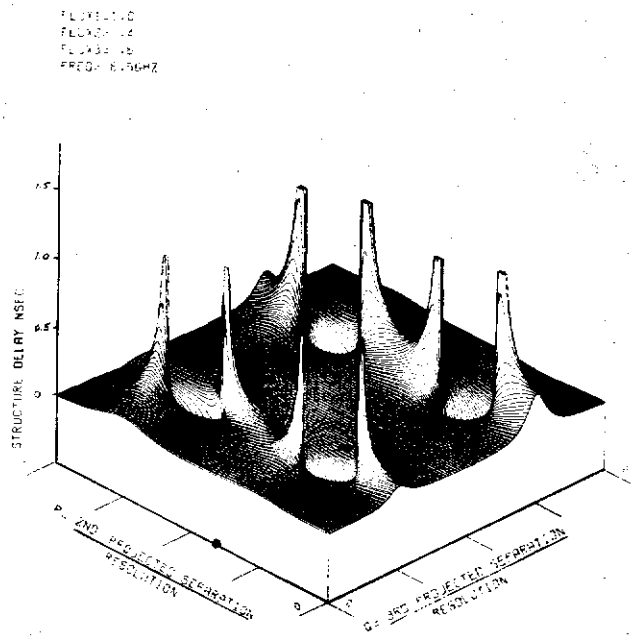

Figure 14. BWS Delay Relative to Brightness Centroid for a Triple-Point Source

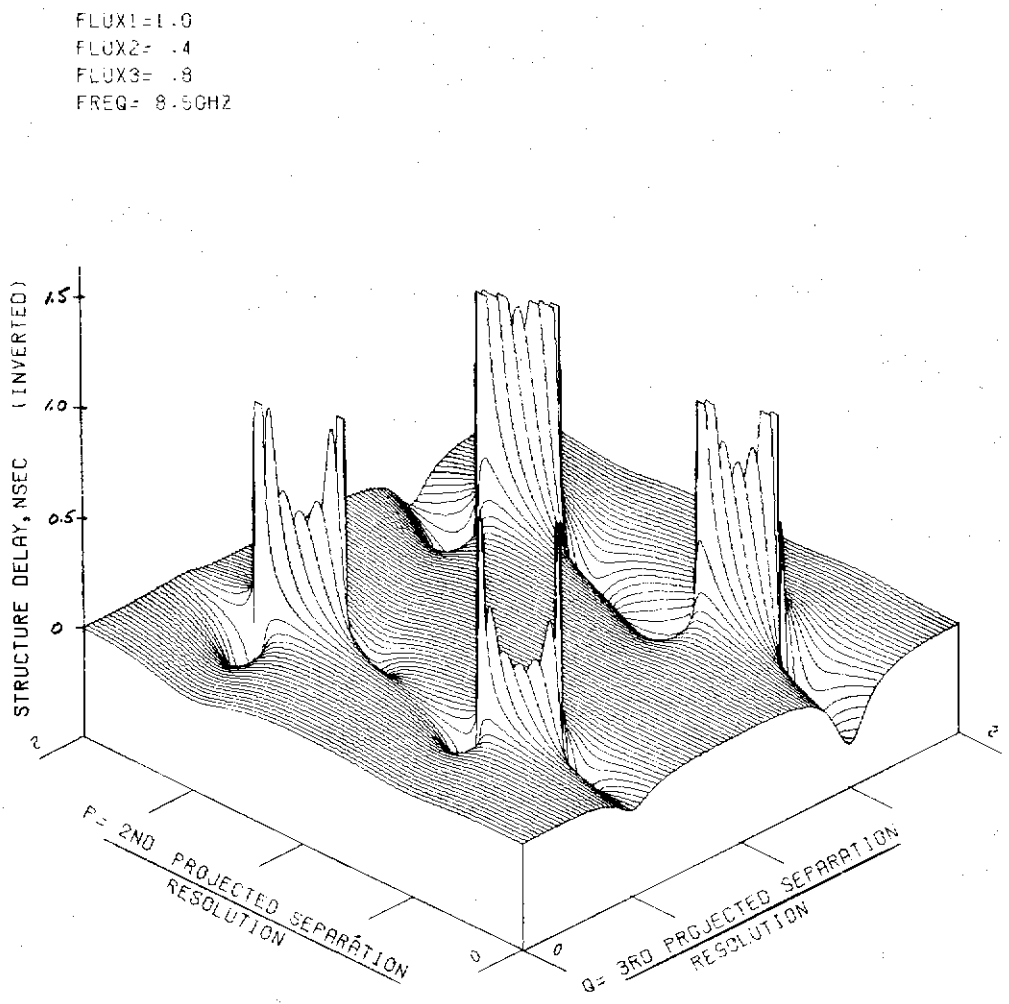

Figure 15. BWS Delay Relative to Brightness Centroid for a Triple-Point Source

QUESTIONS AND ANSWERS

DR. ALLEY:

Where is worldwide time synchronization at the level of the 1/10 nanosecond readily available, because this assists in the unraveling of the source structure of the interferometry measurement.

DR. THOMAS:

Yes it might, but there are better ways to approach that problem. One of the bests tests for approaching whether the theory presented here will be useful in correcting for source structure is to do differential measurements between close adjacent pairs of sources and that way all the typical error sources in VLBI cancel out except for a very few minor ones and then you can look at the actual variations in delay at a very accurate level and can take measurements of brightness distributions to predict what those variations are and see if you get the same results. So we plan to try things like that, if possible, to check our structure calculations. Otherwise, the structure effects tend to get messed up in all of your other error sources in normal interferometry.

DR. TOM CLARK, NASA, Goddard

I just had a couple of brief comments, Brooks. First of all, the information that you show proves that one man's signal is another man's noise, because exactly the same source structure that poses problems in things like clock synchronization or geodesy is exactly what is of interest to the radio astronomer who wants to study these same objects for his other purposes.

One of the things which you might want to stress is that the typical VLBI observation, as was pointed out by Larry Young in his comments and so forth, does not involve just a single source or complex source whatever, but tends to involve anywhere from a half a dozen upwards of 50, depending upon the nature of the observing program, a number of sources on the sky. And although Nature may be a bitch and conspire against you on one source, the chances that she will also be conspiring against you on eight others at the same time is very small. So, in a real experiment, I think these, effects tend to go down much smaller.

There is one other thing which can be done in this to improve the situation and give you additional information. You, of course, pointed out that when the amplitude goes to zero that is the time at which the phase becomes undefined, hence the derivative of phase with respect to frequency becomes undefined and you can't define aproctolae when there are no fringes. That is sort of the summary.

One thing which you can also do at that time is if you are running an interferometer with more than two stations, let us say three, by summing the observed phases around the loop of three stations, all of the instrumental phases cancel out, but the structure phase, at least in its total, around the loop, is still unobservable, so by looking at the closure phase on a three-station interferometer, you can immediately pinpoint when you are having the bad apples problems that can foul up clock synchronization.

DR. THOMAS:

Okay. That is true. One has to be careful though, there may be cases when one wants to do clock synch with not many, many sources but maybe one or two and you want to go out and take a quick measurement of some sort with some limited antenna system or whatever. So it is not always true with clock synch you are going to have 50 sorters or so. It could be a case where you run with only one or two. And also with clock synch. I am not sure that there would always be the funds available to do a closure experiment with three antennas. I suspect it would be a lot more limited effort than that, where you will have a couple of antennas out just to do a clock synch between the stations in question. So, I mean, while your comments are true, I think they might be of limited use.